〈Regular Article〉

RT-LAMP detection method for SARS-CoV-2

Ippei MIYATA[1]，Kazunobu OUCHI[2]

1) Department of Pediatrics, Kawasaki Medical School
2) Department of Medical Welfare for Children, Faculty of Health and Welfare, Kawasaki University of Medical Welfare

ABSTRACT　The COVID-19 (coronavirus disease 2019) pandemic is still endangering the globe since its emergence in December 2019. The authors sought to develop a feasible method to detect RNA of the causative virus, SARS-CoV-2 (severe acute respiratory syndrome corona virus 2), using RT-LAMP (reverse transcription loop-mediated isothermal amplification). The primers designed by the authors successfully detected *in vitro* transcribed RNA sequence (a portion from the surface glycoprotein coding sequence) at an estimated concentration of 16 copy per 20 μL reaction when used with fluorescence detection combined with melting curve analysis; 16 copy per 25 μL reaction when used with a real-time turbidimeter or end-point visual confirmation by the naked eye or fluorescence under UV illumination. Though not tested against actual viral RNA or clinical specimens, this method can serve as another option for rapid detection of the plague-causing virus. Taking into account the feasibility of LAMP, this method may prove its utility especially in resource-limited conditions.

INTRODUCTION

Emerging in December 2019[1], infections caused by SARS-CoV-2 have become an ongoing pandemic. Since its emergence, many methods for detecting the causative virus or obtaining proof of its infection have been sought throughout the globe. As of August 16th, 2021, more than 670 tests are on the market[2]. Still, no single test is flawless. Generally, nucleic acid amplification tests (NAATs) − mostly PCR based − and lateral flow immunoassay tests are the choice for rapid diagnosis of viral infections. NAATs, carried out properly in an ideal condition, exhibits excellent sensitivity and specificity. However, this excellent characteristic also turns out as a vulnerability; even trace contamination of positive material can cause false positive results; nuclease (RNase/DNase) contamination can cause false negative results; thermal calibration of thermal cyclers is also indispensable for reliable and reproducible results. Carried out in small reaction volumes, proper pipetting techniques and calibrated liquid handling devices are required. Therefore, trained professionals, thorough nuclease contamination control, calibrated apparatus, and

Corresponding author
Ippei Miyata
Department of Pediatrics, Kawasaki Medical School,
577 Matsushima, Kurashiki, 701-0192, Japan

Phone : 81 86 462 1111
Fax : 81 86 464 1038
E-mail: miyata.kkcl@gmail.com

dedicated laboratory environment are prerequisites for successful testing at peak performance. Furthermore, nucleic acid extraction from clinical specimens also requires extra time which results in extended turnaround time; whereas time-saving crude extraction is carried out at the cost of potential introduction of impurities/contaminants that might reduce test sensitivity/specificity. In contrast to NAATs, lateral flow immunoassay tests are more inexpensive, can be carried out more easily by less trained professionals. However, the drawback is that immunoassay tests are less sensitive than NAATs.

LAMP is an isothermal nucleic acid amplification method developed in Japan[3]. It uses four primers, which correspond to six short sequences in the target sequence. LAMP requiring six regions of target sequence whereas conventional PCR require two regions, hydrolysis fluorescent probe based real-time PCR ("TaqMan" format) require three, FRET based real-time PCR ("HybProbe" format) require four, chances of mutations introduced into primer/probe annealing sites might be somewhat higher for LAMP than PCR based method, which might reduce amplification efficiency. LAMP does not require costly thermal cyclers, and positive reaction can be determined by the naked eye[4, 5] without the help of costly fluorescent probes used in real-time PCR, which are features advantageous in resource-limited conditions. Taking these characteristics into consideration, LAMP provides a platform for feasible NAAT, more sensitive than lateral flow immunoassays tests, yet less demanding and inexpensive than PCR based methods. Thus, the authors sought to develop a RT-LAMP based method to enable feasible detection of SARS-CoV-2.

MATERIALS AND METHODS
Primers for RT-LAMP
A number of primers were designed with the aid of PrimerExplorer software (https://primerexplorer.

jp/lampv5/index.html). The primers' sequences are shown in Table 1; all but one primer, which was adopted partway through (RevC), were designed by the aforementioned software.

Positive controls
As described elsewhere[6], with no clinical specimens or cultured virus being available at the time, the authors transcribed a portion of genomic sequence of the virus genome coding the surface glycoprotein ("spike protein"), corresponding to nucleotides 24199-25051 of MN908947.3, *in vitro* to serve as an alternative positive control. Diluted RNA of 1×10^3 copies/μL was used for screening candidate inner primers; $1 \times 10^{2/1.5/1}$ copies/μL for screening candidate outer primers and loop-primers. When determining detection limits of finally selected primer sets, 2-fold serial dilutions were prepared *ad hoc*; in this case, reaction of trace concentrations were carried out in multiplicates.

RT-LAMP REACTIONS
Two methods employing different chemistry and apparatus were tested.

Method A
Initial screenings of candidate inner primers were carried out with this method.

This method used Loopamp RNA/DNA Amplification Reagent D (Eiken Chemical Co. Ltd., Tokyo, Japan), in a fixed final reaction volume of 25 μL; this reagent is provided as 8-strip PCR tubes with individual caps attached, with reagents lyophilized inside the tube caps. Reactions were carried out on Loopamp Realtime Turbidimeter LA-500 (Eiken).

Positive reactions turn slightly turbid, yield fluorescence by UV (or blue LED light) irradiation, and change color from pale orange to light green under natural light, enabling visual discrimination by the naked eye (Fig. 1). Calcein (bound with

Table 1. Oligonucleotides employed in this study

Name	Sequence (5'→3')	corresponding positions[*]
Inner Primers		0.235
FIPa	TGCTGACTGAGGGAAGGACATAAGA-	24730-24706
	TGTCAGAGTGTGTACTTGGACA	/ 24648-24669
FIPb	TGCTGACTGAGGGAAGGACATAAGA-	24730-24706
	GTCAGAGTGTGTACTTGGACAA	/ 24649-24670
BIPa	TGGTGTAGTCTTCTTGCATGTGACT-	24736-24760
	TCATGACAAATGGCAGGAGC	/ 24813-24794
BIPb	TGGTGTAGTCTTCTTGCATGTGACT-	24736-24760
	ATCATGACAAATGGCAGGAGC	/ 24814-24794
Outer Primers		
F3	AGAGCTGCAGAAATCAGAGC	24602-24621
B3a	TTCACGAGGAAAGTGTGCTT	24838-24819
B3b	CCTTCACGAGGAAAGTGTGC	24840-24821
B3c	ACCTTCACGAGGAAAGTGTG	24841-24822
RevC	AACCAGTGTGTGCCATTTGA	24870-24851
Loop Primers		
Set H		
LF-H	AGCCCTTTCCACAAAAATCAACTCT	24701-24677
LB-H	TCCCTGCACAAGAAAAGAACTTCAC	24765-24789
Set M		
LF-M	GCCCTTTCCACAAAAATCAACTCTT	24700-24676
LB-M	GTCCCTGCACAAGAAAAGAACTTC	24764-24787
Set L		
LF-L	GATAGCCCTTTCCACAAAAATCAAC	24704-24680
LB-L	CCTGCACAAGAAAAGAACTTCAC	24767-24789

LAMP inner primers consist of two regions (F1c followed by F2, B1c followed by B2) connected as one; their sequences are separated by a hyphen, their corresponding positions are separated by slashes in this table.
Finally selected primers' names are underlined.
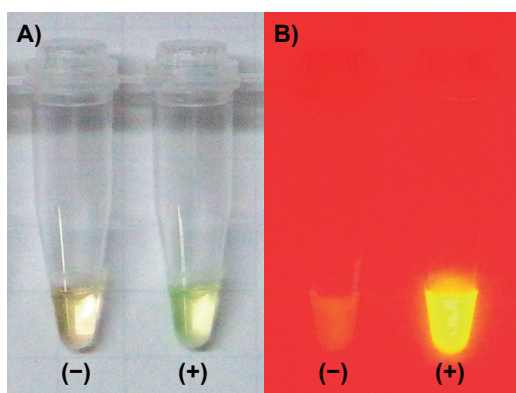[*] according to Reference sequence MN908947.3

Fig. 1. Example of visual discrimination in Method A. (+), positive reaction; (−), negative reaction; Panel A) under ambient fluorescent room light; B) transilluminated by blue LED through dichroic filter, viewed through red filter.

Mn^{2+}) included in the reagent is the fluorescence source, which emits fluorescence as Mn^{2+} (which acts as a fluorescence quencher) is deprived of calcein and further replaced by Mg^{2+}. In LAMP reactions, Mn^{2+} and pyrophosphate ions ($P_2O_7^{4-}$), supplied from dNTPs as they are incorporated into the elongating DNA strand, form manganese pyrophosphate ($Mn_2P_2O_7$) sediments, giving rise to fluorescence[5]. Furthermore, as DNA polymerization proceeds, Mg^{2+} in the reaction buffer forms magnesium pyrophosphate ($Mg_2P_2O_7$) sediments in the same manner, also resulting in turbidity of positive reactions[4].

For transillumination by blue LED, LED505-TR60W Transilluminator (MeCan Imaging Inc.,

Saitama, Japan) was used with consumer product digital cameras.

Method B

This method used WarmStart LAMP Kit (DNA & RNA) (New England Biolabs, MA, USA), in a final reaction volume of 20 μL. Reactions were carried out on CFX96 Detection System (Bio-Rad Laboratories, Hercules, CA, USA). Real-time isothermal amplification was carried out as repetitions of a 7-second single step incubation followed by an approximately 13-second plate read, which resulted in an approximately 20-second incubation. This repetition was preceded by a 2-minute incubation to wait until the hot-lid reached 70℃, when the apparatus become ready for plate reading.

Positive reactions also turn turbid and yield fluorescence. However, the fluorescence exhibited in this method is derived from fluorescent dye intercalating with double stranded DNA, which enables melting curve analysis for further analysis

of the amplified product. For this purpose, a melting curve analysis procedure, consisting of 5 sec incubations from 70℃ up to 95℃ in 0.5℃ increments followed by fluorescence reads, was appended after the amplification cycles and heat inactivation of the enzymes.

Visual discrimination was omitted, since white well plates were used instead of transparent tubes to provide higher fluorescent signals and better S/N ratio.

The finally determined reaction conditions are shown in Table 2 and Fig. 2.

Table 2. Concentration of oligonucleotides for each method

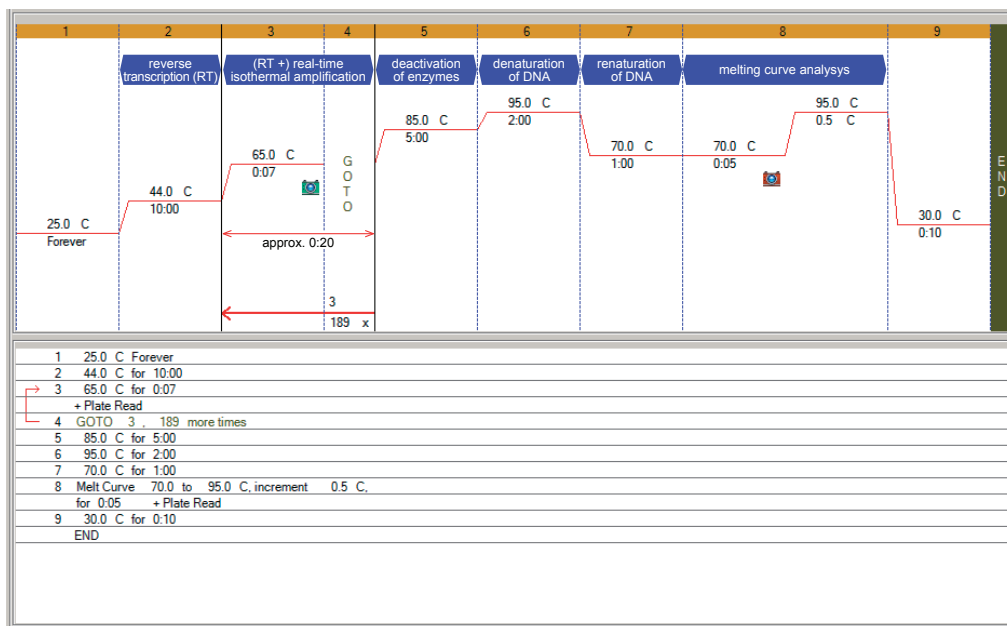| Name	Method A	Method B [μM]
Inner Primers		
FIPb	1.6	1.8
BIPb	1.6	1.8
Outer Primers		
F3	0.2	0.2
RevC	0.4	0.2
Loop Primers		
LF-H	0.4	0.45
LB-H	0.4	0.45

Fig. 2. Reaction conditions for Method B.
Screenshot from actual apparatus with author comments describing each step.

Confirmation of amplified DNA by agarose gel electrophoresis, known to produce a ladder pattern, was not adopted to avoid laboratory contamination from amplified products.

RESULTS

Among the four inner primer combinations combined with three outer primer sets initially evaluated at 62.5℃, only combinations including forward inner primer FIPb exhibited amplification (Fig. 3). The combination of primers FIPb, BIPb, F3, B3a, resulted in the fastest detection, and was subjected to further evaluation for optimal reaction temperature and loop-primer designing/testing. The optimal reaction temperature was determined as 64.0℃. Among the three loop-primer sets further designed to go with this primer set, loop-primer set "H" resulted in the fastest detection and was adopted for further evaluation (data not shown). These primers altogether were selected as our initial primer set.

However, regardless of the methods and/or condition tuning, this initial primer set failed to amplify template RNA less than 5×10^2 copies/reaction. The template RNA being a plus-strand ssRNA, the authors tried the following tuning expecting an increased chance of first strand cDNA reverse transcription initiating from B3 primer and/or BIP: 1) increase B3 primer and/or BIP, 2) try pre-incubation at a temperature allowing RTase activity while not allowing *Bst* DNA polymerase activity. All these attempts failed to make drastic improvements. Noticing that the B3 primer shared approximately half of its sequence with a primer that exhibited the least successful detection (corresponding to nucleotides 24849-24829 of MN908947. 3) in the development of a real-time RT-PCR detection method for SARS-CoV-2[6] that was ongoing in parallel with this study, the authors adopted a primer that exhibited a better detection limit in the development of RT-PCR based detection
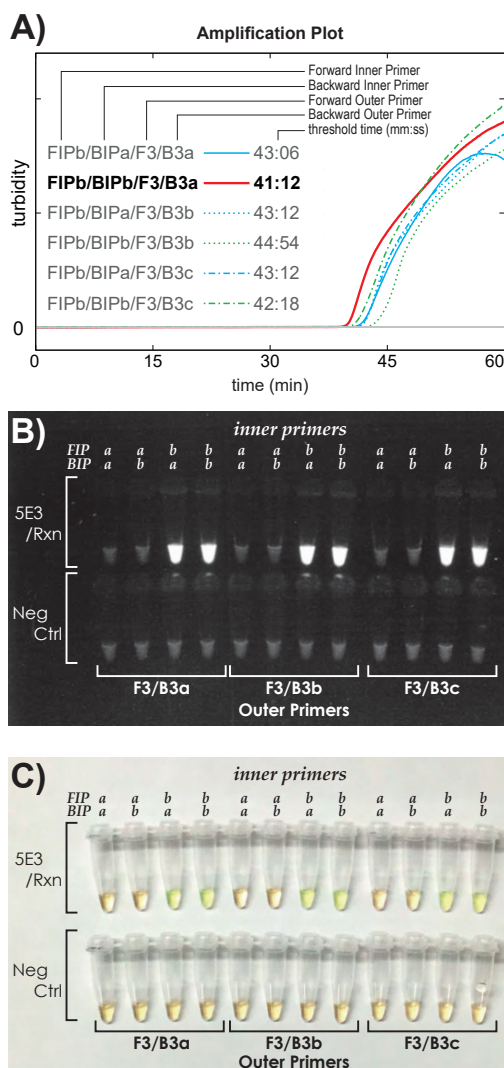

Fig. 3. Screening results for Inner and Outer Primers
Reactions were carried out at 62.5℃ for 60min. For each combination of Forward Inner Primer, Backward Inner Primer, and Outer Primer set, a positive control reaction (5 $\times 10^3$ copies/reaction) and a negative control (RT-PCR grade water) reaction was prepared; Panel A) amplification plots on real-time turbidimeter, threshold times of positive reactions are noted; Panel B) confirmation of reaction tubes by UV illumination; C) confirmation of reaction tubes under ambient light (naked eye).

− primer RevC − as an alternative B3 primer. This alternation resulted in improved detection limits. The final concentrations using this renewed primer set for each method are enlisted in Table 2; optimal reaction temperature for method A was 64.0℃ for 60

minutes, optimal thermal profiles for method B are shown in Fig. 2.

With method B, unintended rises in fluorescence were frequently observed. However, these false negative rises were discriminable from true positive reactions by melting curve analysis; true positive reactions exhibited a melting point of 82.5-83.0℃, whereas false negatives' melting points were 83.5℃ or higher (Fig. 4).

Both methods resulted in similar detection limits; 16 copies per reaction were detectable in triplicated reactions. End point results for method A were concordant with visual evaluation (Fig. 5).

DISCUSSION

We have succeeded in developing a real-time RT-LAMP method to detect SARS-CoV-2 RNA sequence. Though a number of real-time RT-PCR methods[7, 8] as well as LAMP based methods[9-11] have been reported in the literature, we have developed yet another potent tool for detection of the virus.

The authors tested two different detecting methods. Detection using real-time turbidimeter and/or endpoint visual determination (Method A) resulted in a detection limit of 16 copies per 25 μL reaction. This detection limit is no less than better to the domestically approved LAMP based *in vitro* diagnosis (IVD) kit, whose detection limit is referred to as 60 copies per 25 μL reaction in its package insert[11]. Clear visual determination was also feasible (Fig. 1, 5), since negative control reactions remained negative. The reagent takes the form of an amplification reaction tube with buffer, dNTP, and enzymes lyophilized inside the tube cap stored at room temperature. Thus, preparing the reactions was simple and time required was short; apply primer mixture, template solution and water to the tube. Chances of errors and cross-contaminations were also reduced due to fewer tubes and fewer reagents on the benchtop.
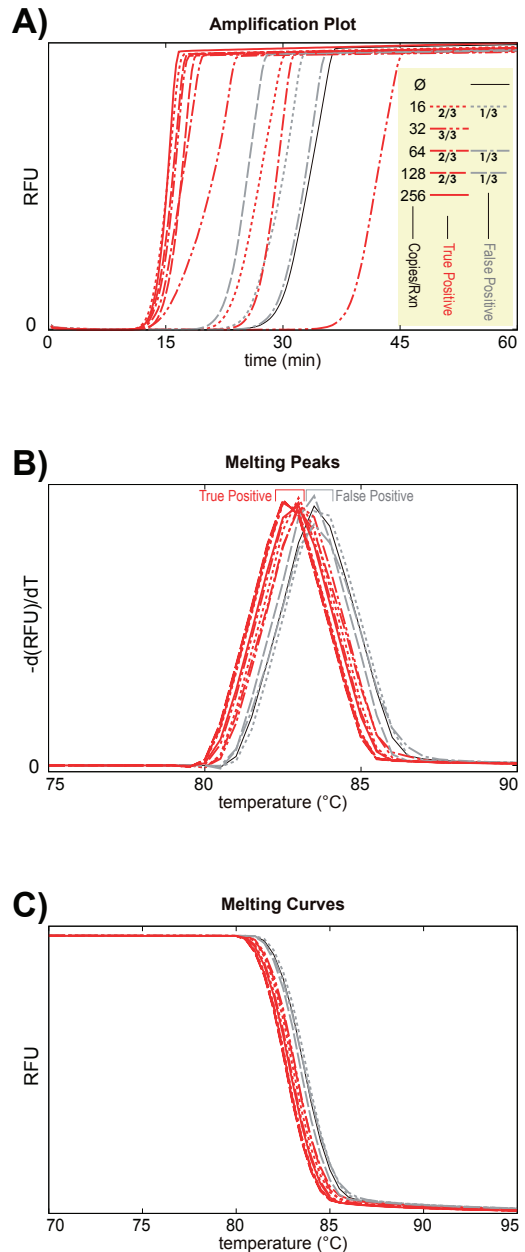
Fig. 4. Detection limit determination in Method B
RFU, relative fluorescence unit; Rxn, reaction; styles of thick lines and the estimated template concentrations (copies/reaction) each style represent are－solid, 256; dashed, 128; dot-dashed, 64; dot-dot-dashed, 32; dotted, 16; red thick lines represent reactions determined as true positive, whereas gray represent false positives; thin black solid lines represent negative (no template) controls; Panel A) amplification plot, number of true/false positives among multiplicates are denoted under the legend; B) melting curve analysis; C) melting peaks.

A)

Amplification Plot

copies/Rxn		threshold time (mm:ss)
ø		
8		
16	26:12	
32	29:54, 27:18	
64	32:48, 43:54, 25:18	
128	19:48, 20:30, 41:36	

turbidity

time (min)

B)

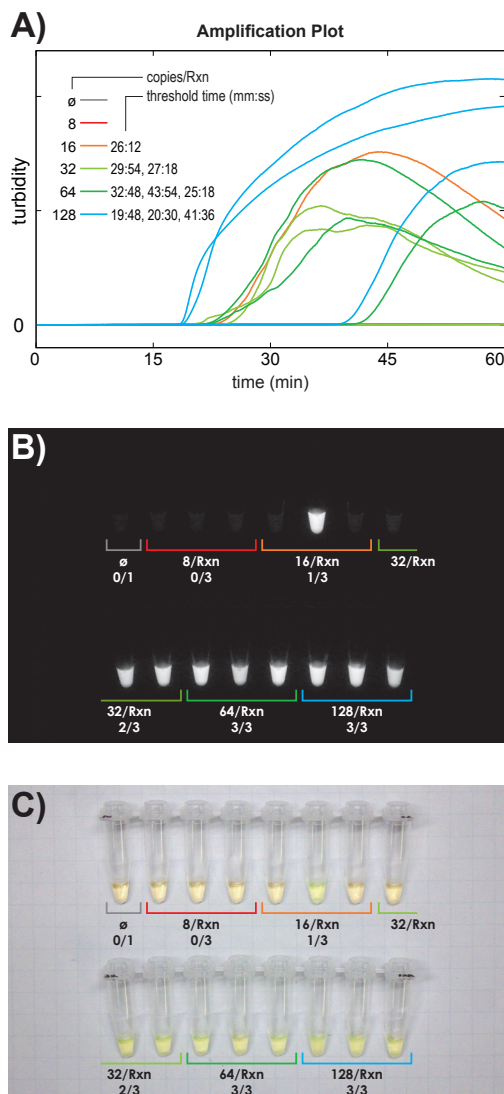| ø	8/Rxn	16/Rxn	32/Rxn
0/1	0/3	1/3	

32/Rxn	64/Rxn	128/Rxn
2/3	3/3	3/3

C)

ø	8/Rxn	16/Rxn	32/Rxn
0/1	0/3	1/3	

32/Rxn	64/Rxn	128/Rxn
2/3	3/3	3/3

Fig. 5. Detection limit determination in Method A
Reactions were carried out at 64.0℃ for 60min. Negative (no template) control reactions are denoted as ø; Panel A) amplification plots on real-time turbidimeter, threshold times of positive reactions are noted; B) confirmation of reaction tubes by UV illumination; C) confirmation under ambient room light (fluorescent light).

Furthermore, more template solution (i.e., more total target molecules) can be applied to one reaction, which is another potential benefit compared to other kits provided with concentrated aqueous solutions of buffer, dNTP and enzymes; this feature boosts the chance of detecting trace amount of target sequence in the template solution.

Detection on a real-time PCR apparatus (Method B) was capable of detecting 16 copies per 20 μL reaction (Fig. 4). However, fluorescent signals were detected from negative control reactions, requiring additional melting curve analysis for discrimination of unintended false negative results from true positive amplifications. The reagent being a $2 \times$ premix of buffer, dNTP, "WarmStart" DNA polymerase and reverse transcriptase, the reaction could be rapidly and feasibly set up at room temperature with less complexities than conventional kits. The flexible reaction volume is also advantageous when less reaction volume is preferred, e.g. limited available specimen volumes, glass capillary based thermal cyclers, 384-well plates, and cost saving demands. However, melting curve analysis requires additional time, as well as costly detection apparatus for precise temperature control and fluorescence reading.

Both modes of detection resulted in similar detection limits. However, the optimal reaction temperature and primer concentrations differed between the amplification kits. Practitioners should be aware of such potential differences that can affect test performance when adopting LAMP primer sets from the literature; deliberate preliminary experiments are strongly recommended in such situations to avoid unintended amplification (false positives) as well as aggravated detection limits (false negatives).

Another interesting finding regarding first strand cDNA transcription was that outer primers for RT-LAMP might share features with RT-PCR primers targeting the same sequence. Our initially designed three B3 primers that shared approximately half of the sequence with an unsuccessful RT-PCR primer were also unsuccessful, while the B3a primer that shared the least number of nucleotides proved to be the best among the three. In contrast, a successful RT-PCR primer adopted without modification to

Table 3. Characteristic amino acid alterations in surface glycoprotein (spike protein) of variants of concern (VOC)

VOC	
α (alpha)	H69del, V70del, Y144del, N501Y, A570D, D614G, P681H, T716I, S982A
β (beta)	D80A, D215G, L242del, A243del, L244del, K417N, E484K, N501Y, D614G, A701V
γ (gamma)	L18F, T20N, P26S, D138Y, R190S, K417T, E484K, N501Y, D614G, H655Y, T1027I
δ (delta)	T19R, T95I, G142D, E156-, F157-, R158G, L452R, T478K, D614G, P681R, D950N

```
MFVFLVLLPL VSSQCVNLTT RTQLPPAYTN SFTRGVYYPD KVFRSSVLHS TQDLFLPFFS    60

NVTWFHAIHV SGTNGTKRFD NPVLPFNDGV YFASTEKSNI IRGWIFGTTL DSKTQSLLIV   120

NNATNVVIKV CEFQFCNDPF LGVYYHKNNK SWMESEFRVY SSANNCTFEY VSQPFLMDLE   180

GKQGNFKNLR EFVFKNIDGY FKIYSKHTPI NLVRDLPQGF SALEPLVDLP IGINITRFQT   240

LLALHRSYLT PGDSSSGWTA GAAAYYVGYL QPRTFLLKYN ENGTITDAVD CALDPLSETK   300

CTLKSFTVEK GIYQTSNFRV QPTESIVRFP NITNLCPFGE VFNATRFASV YAWNRKRISN   360

CVADYSVLYN SASFSTFKCY GVSPTKLNDL CFTNVYADSF VIRGDEVRQI APGQTGKIAD   420

YNYKLPDDFT GCVIAWNSNN LDSKVGGNYN YLYRLFRKSN LKPFERDIST EIYQAGSTPC   480

NGVEGFNCYF PLQSYGFQPT NGVGYQPYRV VVLSFELLHA PATVCGPKKS TNLVKNKCVN   540

FNFNGLTGTG VLTESNKKFL PFQQFGRDIA DTTDAVRDPQ TLEILDITPC SFGGVSVITP   600

GTNTSNQVAV LYQDVNCTEV PVAIHADQLT PTWRVYSTGS NVFQTRAGCL IGAEHVNNSY   660

ECDIPIGAGI CASYQTQTNS PRRARSVASQ SIIAYTMSLG AENSVAYSNN SIAIPTNFTI   720

SVTTEILPVS MTKTSVDCTM YICGDSTECS NLLLQYGSFC TQLNRALTGI AVEQDKNTQE   780

VFAQVKQIYK TPPIKDFGGF NFSQILPDPS KPSKRSFIED LLFNKVTLAD AGFIKQYGDC   840

LGDIAARDLI CAQKFNGLTV LPPLLTDEMI AQYTSALLAG TITSGWTFGA GAALQIPFAM   900

QMAYRFNGIG VTQNVLYENQ KLIANQFNSA IGKIQDSLSS TASALGKLQD VVNQNAQALN   960

TLVKQLSSNF GAISSVLNDI LSRLDKVEAE VQIDRLITGR LQSLQTYVTQ QLIRAAEIRA  1020

SANLAATKMS ECVLGQSKRV DFCGKGYHLM SFPQSAPHGV VFLHVTYVPA QEKNFTTAPA  1080

ICHDGKAHFP REGVFVSNGT HWFVTQRNFY EPQIITTDNT FVSGNCDVVI GIVNNTVYDP  1140

LQPELDSFKE ELDKYFKNHT SPDVDLGDIS GINASVVNIQ KEIDRLNEVA KNLNESLIDL  1200

QELGKYEQYI KWPWYIWLGF IAGLIAIVMV TIMLCCMTSC CSCLKGCCSC GSCCKFDEDD  1260

SEPVLKGVKL HYT        1273
```

Legends

Amino Acid residues

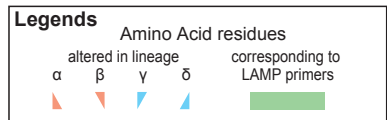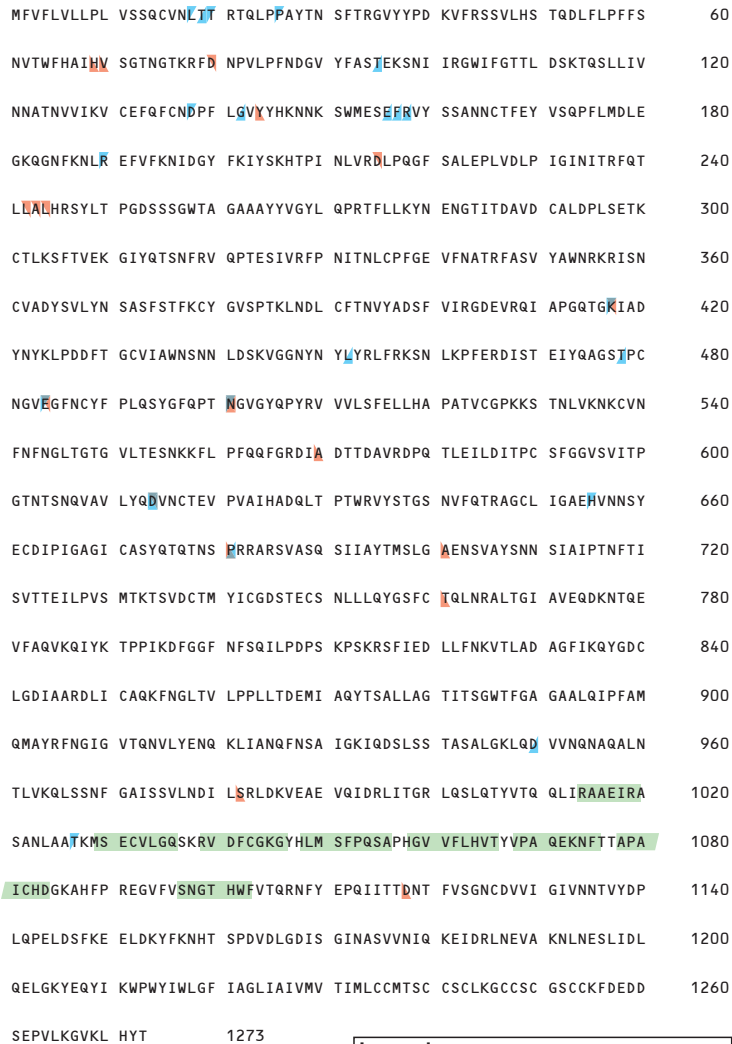| altered in lineage	corresponding to
α β γ δ	LAMP primers

Fig. 6. Illustration of characteristic amino acid changes of VOCs' and amino acid positions corresponding to LAMP primer annealing sequences.

Amino acid (AA) residues of the surface glycoprotein are represented in one letter IUPAC abbreviations (RefSeq MN908947.3). Orthogonal triangles with the right angle at the lower left (red) indicate altered AA residues in lineage α (alpha); upper right (red), lineage β (beta); upper left (cyan), lineage γ (gamma); lower right (cyan), lineage δ (delta). Green backgrounds indicate AA residues corresponding to LAMP primer annealing sequences.

replace the unsuccessful B3a primer also yielded good results in RT-LAMP. The unsuccessful primers were located in a relatively GC-rich sequence, whereas the successful primers were in an AT-rich sequence; higher-order RNA structure might have played a role in this difference. Based on this finding, though actual experiments have yet to be conducted, RT-LAMP outer primer selection may be supplemented by prior RT-PCR experiments to screen candidate primers or primer binding sites.

Many variants of the causative virus have been identified and reported since its emergence. In general, amplification efficiency might be reduced, should mismatch occur in annealing positions of primers utilized in nucleic acid amplification. As of July 2021, the lineages enlisted in Table 3 are regarded as variants of concern (VOC) by the Japanese National Institute of Infectious Diseases[12]. The VOCs' characteristic amino acid (AA) alterations[13] within the surface glycoproten are summarized in Table 3; positions of these AAs, along with AAs corresponding to our LAMP primers' annealing sequences are illustrated in Fig. 6. As demonstrated in Fig. 6, the alterations characteristic of VOC's do not overlap with those corresponding to the LAMP primers. Therefore, impairment of our LAMP method's detection performance is unlikely to be caused by the alterations enlisted in Table 3.

The authors are aware of the following limitations. Actual viral RNA controls could not be carried out, due to inaccessibility. But a few clinical specimens assessed by this method at the early stage of the pandemic all proved negative, concordant with PCR-based evaluation. Furthermore, specificity studies employing nucleic acid extracts derived from clinical specimens known to be positive for other causative agents of respiratory infections could not be carried out due to time-consuming procedures to abide by institutional ethical policies. Evaluations utilizing such clinical specimens are needed.

The pandemic caused by SARS-CoV-2 is still causing chaos all over the globe. Many feasible tests are available, but no single method is perfect. Our LAMP based method may serve as another complementary method to detect this plague-causing virus, especially in resource-limited situations/countries.

In conclusion, we have succeeded in developing a Real-Time RT-LAMP detection method for SARS-CoV-2 with detection limits no less than better to the domestically approved LAMP based IVD kit, which could prove useful in resource-limited situations/countries.

ACKNOWLEDGEMENTS

CONFLICT OF INTEREST

None.

REFERENCES

1 ） https://www.who.int/emergencies/disease-outbreak-news/item/2020-DON229 (2021. 8. 16)

2 ） https://finddx.org/test-directory/ (2021. 8. 16)

3 ） Notomi T, Okayama H, Masubuchi H, Yonekawa T, Watanabe K, Amino N, Hase T: Loop-mediated isothermal amplification of DNA. Nucleic Acids Res. 2000; 28: e63. doi: 10.1093/nar/28.12.e63.

4 ） Mori Y, Nagamine K, Tomita N, Notomi T: Detection of loop-mediated isothermal amplification reaction by turbidity derived from magnesium pyrophosphate formation. Biochem Biophys Res Commun. 2001; 289: 150-154. doi: 10.1006/bbrc.2001.5921.

5 ） Tomita N, Mori Y, Kanda H, Notomi T: Loop-mediated isothermal amplification (LAMP) of gene sequences and simple visual detection of products. Nat Protoc. 2008; 3: 877-882. doi: 10.1038/nprot.2008.57.

6 ） Miyata I, Ouchi K: Real-time RT-PCR detection method

for SARS-CoV-2. Kawasaki Med J. 2020; 46: 97-101. doi: 10.11482/KMJ-E202046097.

7 ） https://www.niid.go.jp/niid/images/lab-manual/2019-nCoV20200225.pdf (2021. 8. 16) (Article in Japanese)

8 ） Corman VM, Landt O, Kaiser M, *et al.*: Detection of 2019 novel coronavirus (2019-nCoV) by real-time RT-PCR. Euro Surveill. 2020; 25: 2000045. doi: 10.2807/1560-7917.ES.2020.25.3.2000045.

9 ） Thompson D, Lei Y: Mini review: Recent progress in RT-LAMP enabled COVID-19 detection. Sensors and Actuators Reports. 2020; 2: 100017. doi: 10.1016/j.snr.2020.100017.

10） Kitagawa Y, Orihara Y, Kawamura R, Imai K, Sakai J, Tarumoto N, Matsuoka M, Takeuchi S, Maesaki S, Maeda T: Evaluation of rapid diagnosis of novel coronavirus disease (COVID-19) using loop-mediated isothermal amplification. J Clin Virol. 2020; 129: 104446. doi: 10.1016/j.jcv.2020.104446.

11） Eiken Chemical Co. L. Loopamp® Novel Corona Virus 2019 (SARS-CoV-2) Detection Reagent Kit (Package Insert). 2020

12） https://www.niid.go.jp/niid/ja/diseases/ka/corona-virus/2019-ncov/2484-idsc/10554-covid19-52.html (2021. 8. 16) (Article in Japanese)

13） Centers for Disease Control and Prevention. SARS-CoV-2 Variant Classifications and Definitions (Updated Aug. 24, 2021). https://www.cdc.gov/coronavirus/2019-ncov/variants/variant-info.html (2021. 8. 27)